



## Lasers in Manufacturing Conference 2021

# Laser turning using ultra-short laser pulses and intensity distribution techniques

Julian Zettl<sup>a,\*</sup>, Christian Bischoff<sup>b,c</sup>, Stefan Rung<sup>a</sup>, Cemal Esen<sup>c</sup>, Andrés Fabián Lasagni<sup>d</sup> and Ralf Hellmann<sup>a</sup>

<sup>a</sup>*University of Applied Sciences Aschaffenburg, Würzburger Str. 45, 63743 Aschaffenburg, Germany*

<sup>b</sup>*Topag Lasertechnik GmbH, Nieder-Ramstädtner Str. 247, 64285 Darmstadt, Germany*

<sup>c</sup>*Ruhr University Bochum, Universitätsstrasse 150, 44801 Bochum, Germany*

<sup>d</sup>*Technical University Dresden, Large Area Surface Structuring, 01069 Dresden, Germany*

---

### Abstract

We report on micromachining of rotationally symmetric parts using ultra-short laser pulses by a laser turning process. In particular, we compare the application of a focused Gaussian beam shape and a Top Hat beam profile as being generated by a concave freeform beam shaping optical element. The beam-shaping element is placed in the beam path with a specified lateral displacement to create a shifted intensity profile within the focal spot in order to specifically improve the efficiency of the laser turning process. Assessment criteria are the ablation rate and the ablation efficiency. Our study reveals a distinct increase of the process efficiency by using Top Hat beam shaping, which especially for low laser powers amounts to an increase of the ablation rate by about 57 %.

Keywords: ultra-short laser pulses, laser turning, beam shaping, ablation rate, process efficiency;

---

### 1. Introduction

The turning process in general is used to manufacture rotationally symmetric parts with the work piece rotating around its own axis, being mechanically machined by a lathe chisel or an indexable insert. However, this approach holds several disadvantages regarding friction related heat, shear forces and tool wearing.

---

\* Corresponding author.

E-mail address: julian.zettl@th-ab.de

By using focused ultra-short laser pulses to machine the part, this process profits from the cold ablation as well as its non-contact nature. In addition, ultra-short laser pulses allow to machine a great variety of materials such as metals, fused silica, polymers and ceramics (Lickschat et al., 2020, Žemaitis et al., 2019, Schwarz and Hellman, 2017, Canfield et al., 2020, Ravi - Kumar et al., 2019, Yang et al., 2019, Chen et al., 2020).

For the turning process, the focused laser beam is guided alongside the rotating work piece, hence impinging the component at an angular incidence. This specific collocation enables the process to “self-limitation” in terms of material removal, meaning the diameter reduction of the part is solely dependent on the positioning and feeding of the laser beam. The properties and advantages of such a setup have already been shown in a previous study by Zettl et al., 2020.

Beam shaping in laser micro machining with ultra-short laser pulses has previously been employed to benefit from various effects: dividing the beam into several sub-beams by utilizing a spatial light modulator, for instance, can be used to increase the ablation rate, as shown by Lutz et al., 2021. Xie et al., 2016 were able to generate boreholes with an aspect ratio of 330:1 in PMMA, using a Bessel beam shape, generated by an axicon. While using a Gaussian beam profile, the part of the spatial energy distribution that is below the ablation threshold of a particular process, does not contribute to the material removal, yet may lead to unwanted heating of the work piece. Using a more homogeneous intensity distribution of a Top Hat profile, the losses of energy into heating will be reduced and the process can be more efficient (see Fig. 1).

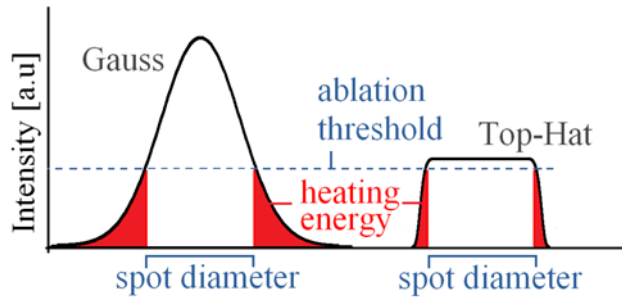


Fig. 1. Depiction of intensity losses into heat Gaussian and Top Hat beam shapes.

For several applications like Matrix-assisted Laser Desorption/Ionization (MALDI), shown by Wiegemann et al., 2016, Direct Laser Interference Patterning (DLIP), demonstrated by El-Khoury et al., 2018, thin film applications, applied by Rung, 2013, Račiukatis et al., 2011 or Laser-Induced Breakdown Spectroscopy (LIBS), as deployed by Basler et al., 2019, it has been shown that the use of Top-Hat beam profiles with uniform energy distribution can also improve the process quality.

Typically, pulsed lasers with a Gaussian beam profile and high power densities are used in laser material micro machining. In order to modify the spatial intensity distribution over the beam profile in the focal plane, the phase of a Gaussian laser beam has to be changed in a controlled manner. It is worthwhile to mention, that not only the intensity profile but also the footprint of the focal spot can be modified, e.g. transforming the footprint of a rotationally symmetric Gaussian profile into a, beside a round footprint, a square or rectangular one, having a Top Hat intensity profile.

Refractive or diffractive optical components can be used to change the phase of a laser beam. Diffractive concepts typically achieve Top Hat profiles close to the diffraction limit of the Gaussian beam, as shown by Veldkamp and Kastner, 1982, Bischoff et al., 2019, Yang and Wang, 2003, and generally do not allow the Top-Hat size to be adjusted independently of the numerical aperture of the focusing system. Refractive concepts for Top Hat beam shaping are flexible and allow the realization of almost any Top Hat size. They lead to continuous phase distributions, which, in the case of round Top Hat profiles, show a distribution  $\phi(r)$  that is

rotationally symmetrical about the optical axis. In the case of square and rectangular Top-Hat profiles the phase distribution can be separated in x and y,  $\phi(x,y)$ . Calculation methods for such phase distributions are given by Hossfeld et al., 1991, Dickey and Holswade, 1996, Romero and Dickey, 1996. For applications in laser processing, the phase profiles determined in this way must be realized as optical elements. These are in the case of  $\phi(r)$  aspheric optical components and in the case of  $\phi(x,y)$  so-called freeform optics.

The resulting height profile of such beam shaping elements can be determined according to Goodman, 1996 as follows:

$$h(x,y) = \frac{\lambda}{2\pi(n-1)} \cdot \varphi(x,y) \quad (1)$$

Where  $\lambda$  is the used wavelength,  $n$  is the refractive index and  $\varphi(x,y)$  is the phase distribution across the optical element. Typical height variations for Top-Hat beam shaping optics for ultra-short pulse laser processing are in the range of a few 10  $\mu\text{m}$ .

In this study, a GTH (Gaussian to Top Hat) concave freeform beam shaping optic is used. This optic is designed for irradiation with a Gaussian beam of radius  $w = 2 \text{ mm}$  at  $1/e^2$ . In order to achieve the best possible Top Hat profile, the centers of the Gaussian beam and of the GTH optic must be positioned very precisely to one another in the range of  $<0.1 \cdot w$ . After passing the GTH optic, the beam was focused by a lens with a focal length of 60 mm.

## 2. Materials and methods

For the evaluation of the laser turning process, stellite rods (quality K-44 UF, 88 % WC, 12 % Co) with an initial diameter of 1.8 mm are chosen. This material has a high flexural strength of  $>4000 \text{ N/mm}^2$  and is commonly used for shaping or drilling cast iron, titanium alloys, stainless steel or high temperature resistant alloys.

The laser system is equipped with three linear movable axes and one rotary axis with a maximum speed of 500 rpm. As laser source, an ultra-short pulse laser system (Carbide CB3-40W, Light Conversion, Lithuania) with a pulse duration of 250 fs and a maximum pulse energy of 0.4 mJ is deployed. The processing head generates a focus spot of 18  $\mu\text{m}$  in diameter and is also able to apply a constant gas flow of approximately 30 l/min through a nozzle orifice of 1 mm. Throughout the experiments, the focal plane of the laser spot is constantly set at the level of the rotation axes.

In order to generate a top hat beam profile in the focal spot, a GTH beam-shaping element was placed within the beam path. The resulting square shaped focal spot has an edge length of 100  $\mu\text{m}$  and a homogeneous intensity distribution inside the focal area. By moving the element sideways, the resulting intensity distribution within the focus shifts accordingly. This lateral displacement of the element allows redistributing the available laser intensity to generate a line-spot like focal area on one side of the original top hat area with a slowly decreasing intensity profile towards the other side (cf. Fig. 3).

This particular intensity profile is subsequently used in the laser turning process as illustrated in Fig. 2. The peak intensity is located 100  $\mu\text{m}$  aside the outer circumference of the work piece, facing towards the material center. The x-axis moves the sample under the laser spot parallel to the rotation axis, realizing the feed rate.

For the simulation of the propagation behavior of the GTH shaped beams, the commercial physical optics software VirtualLab Fusion, running the Classical Field Tracing simulation engine with SPW operator, was used, on a workstation with an AMD Ryzen™ Threadripper™ 2990WX processor, 32 cores, 3GHz and 128GB RAM memory

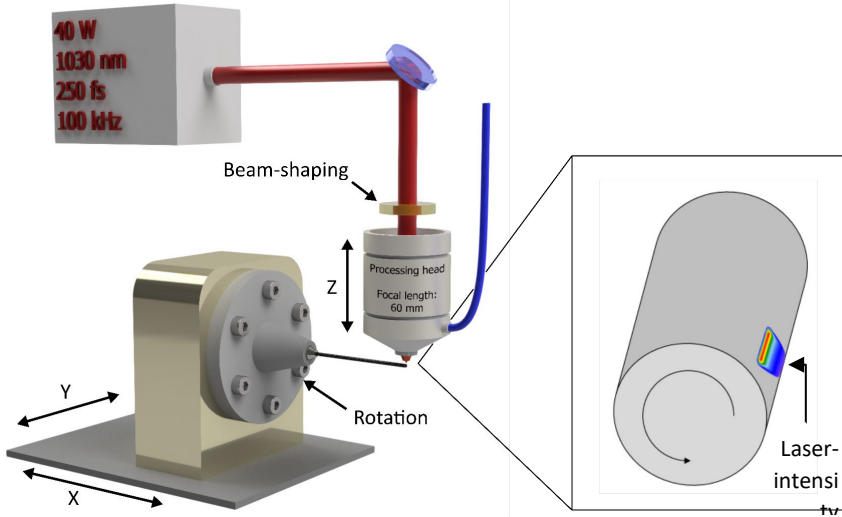


Fig. 2. Process setup for laser turning with beam shaping element.

To quantify the efficiency and the ablation rate of the laser turning process with and without the beam shaping element, the initial diameter  $d_i$  and the final diameter  $d_f$  of the work piece were measured using an optical microscope (Leica DVM6), thus calculating the ablation rate  $\dot{V}$  according to

$$\dot{V} = \left( \left( \frac{d_i}{2} \right)^2 - \left( \frac{d_f}{2} \right)^2 \right) \cdot \pi \cdot \dot{x} \quad (2)$$

where  $\dot{x}$  represents the feeding speed. The process efficiency is calculated by dividing the ablation rate  $\dot{V}$  by the applied average laser power.

### 3. Beam shaping element characteristics

A simulated Gaussian intensity profile in the focal plane of the optical setup (without GTH) is shown in Fig. 3a. By introducing the GTH optic into the beam path, the phase distribution in front of the focusing optic is influenced and the intensity distribution in the focal plane is transformed into a square Top Hat profile, depicted in Fig. 3c. The lateral dimension of the top hat profile is approximately 140x140  $\mu\text{m}^2$  i.e. about 7 times larger than the  $1/e^2$  diameter of the unaffected Gaussian profile of size of approximately 20  $\mu\text{m}$ .

As shown in studies by Dickey and Holswade, 1996, Romero and Dickey, 1996, a lateral shift of such a beam shaping optic in the range  $>0.1 \cdot w$  leads to a tilting of the intensity profile in the focal plane. By increasing the lateral shift in y-direction (cf. Fig. 2), the formerly square Top Hat profile changes into a homogeneous line profile, as shown in Fig. 3e. Cross sections of the corresponding intensity distribution are shown in Fig. 3b, d and f. It is worthwhile noticing that the peak intensity of the Gaussian beam shape is about 40 times larger than the peak intensity of the shifted Top Hat profile for the same input parameters.

Since the maximum feed rate for a continuous ablation in the laser turning process is limited by the rotation speed of the work piece divided by the laser spot size, an elongated line profile is beneficial for the overall process behavior.

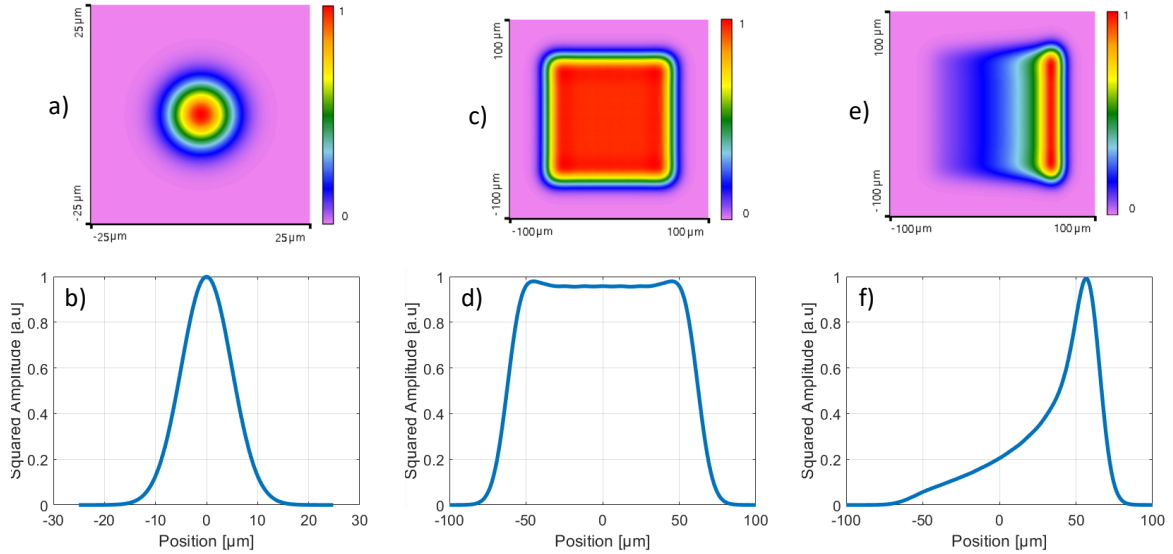


Fig. 3. (a) Intensity distribution of focused Gaussian laser beam, (b) Cross section of focused Gaussian beam, (c) Top Hat intensity distribution, (d) Top Hat cross section, (e) Intensity distribution of shifted Top Hat, (f) Cross section of shifted Top Hat. All intensities are normalized to one to their respective maximum.

In addition to the changed intensity profile in the focal plane, introducing the GTH into the beam path also changes the propagation behavior in front and behind the focal plane. For a better understanding, pictures of the calculated propagation of focused rays are shown in the following Fig. 4 - Fig. 6. To generate these images, several cross-sections of the intensity profile along the x-axis or y-axis are calculated at different positions along the propagation axis z (optical axis) and are composed together. Each displayed image of a calculated propagation is normalized to the maximum intensity. In Fig. 4 the intensity profile for the x-axis along propagation around the focal plane of an ideal focused Gaussian beam with wavelength  $\lambda = 1030$  nm, focal length  $f = 60$  mm and input beam radius  $w = 2$  mm is shown. The intensity distribution of a focused Gaussian beam is rotationally symmetrical to the optical axis, so that the same intensity distribution is present in the z-direction for the y-axis. In addition, the intensity distribution is point symmetrical to the focal spot.

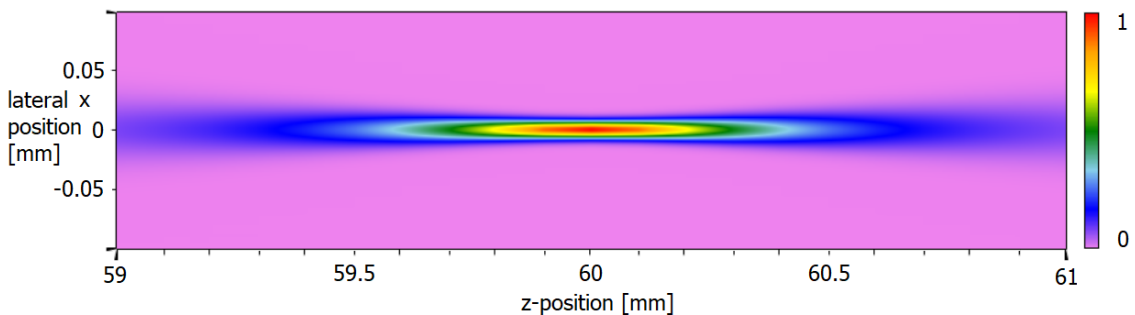


Fig. 4. Caustic of focused Gaussian beam along z-axis for  $z = 59$  mm to  $z = 61$  mm.

Both symmetries are broken by introducing the GTH beam shaping optic. In Fig. 5 (Top) the intensity profile for the x-axis along propagation around the focal plane of the shaped laser beam is shown. Behind the focal plane, the beam size decreases steadily and the Top-Hat profile changes. Selected intensity distributions along the propagation for the positions  $z = 59$  mm, 60 mm and 61 mm are shown in Fig. 5 (Bottom). The optimum

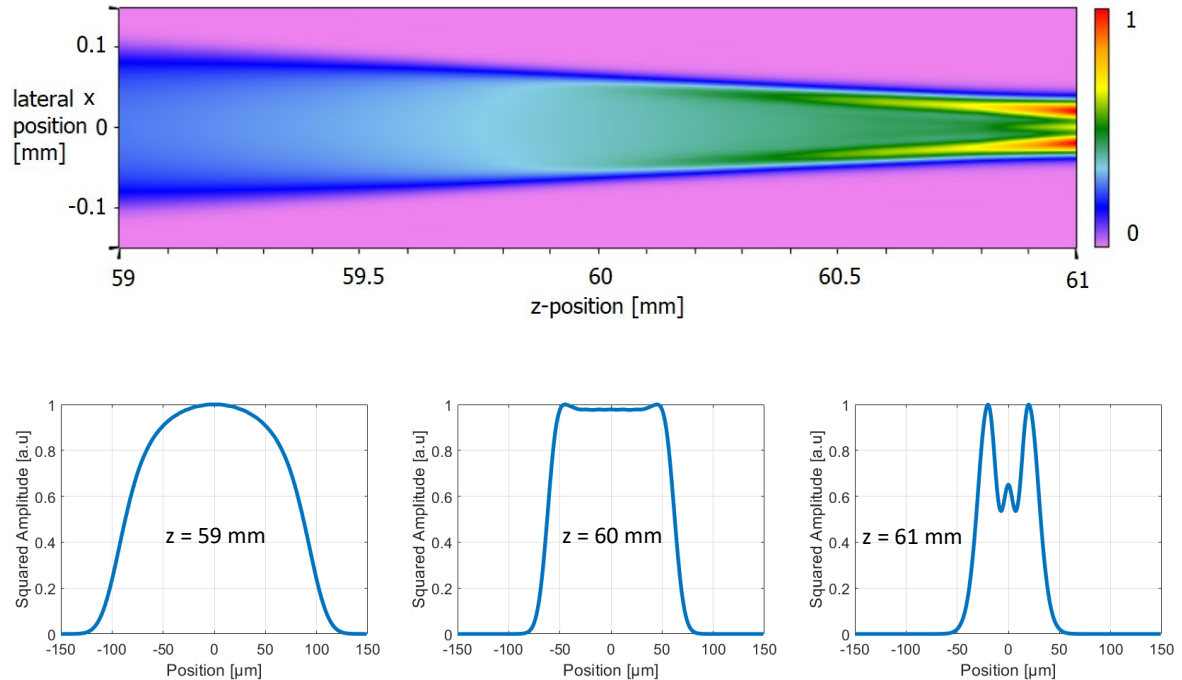


Fig. 5. Top: Caustic of x-axis for GTH shaped laser beam along z-axis for  $z = 59$  mm to  $z = 61$  mm. Bottom: Selected intensity distributions (x-axis) along the propagation for the positions  $z = 59$  mm, 60 mm and 61 mm. All intensities are normalized to one to their respective maximum.

Top Hat profile lies at 60 mm, as shown in Fig. 5 (Bottom, Middle). At  $z = 62.5$  mm, the smallest spot size of around 30  $\mu\text{m}$  with a sinc-like intensity distribution is achieved. The offset of the smallest possible spot can be explained by the fact that the GTH is a concave lens, which leads in combination with the used focusing optic to a longer focal length, as shown by Dickey and Holswade, 1996.

A lateral shift of the GTH optics along the y-axis (cf. Fig. 2), as described above and shown in Fig. 3e) and f), additionally changes the propagation behavior for this axis. Fig. 6 (Top) shows the intensity profile for the y-axis along the propagation around the focal plane of the laser beam formed by a GTH lens shifted by 1 mm. Selected intensity distributions along the propagation for the positions  $z = 59$  mm, 60 mm and 61 mm are shown in Fig. 6 (Bottom).

Depending on the work piece diameter and the processing strategy, the uneven intensity distribution as shown in Fig. 6 (bottom right) needs to be taken into account. In this case, however, due to the given work piece and laser positioning, this behavior is neglectable since the laser propagation irradiates the material surface between 59.59 and 60 mm z-position.

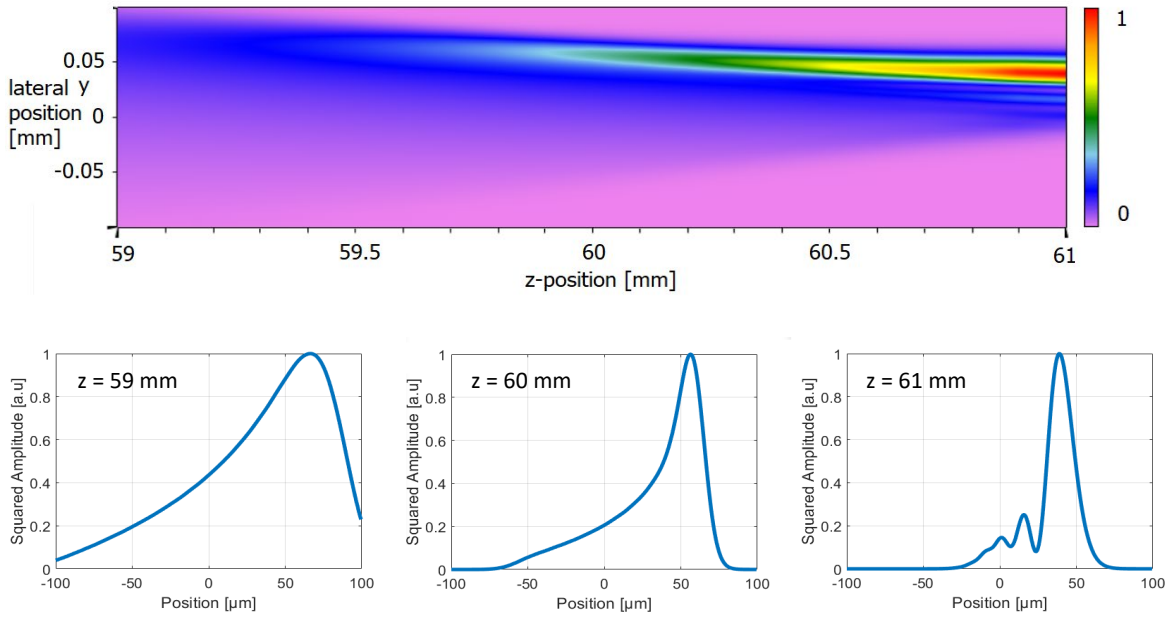


Fig. 6. Top: Caustic for y-axis for shifted GTH shaped laser beam along z-axis for  $z = 59$  mm to  $z = 61$  mm. Bottom: Selected intensity distributions (y-axis) along the propagation for the positions  $z = 59$  mm, 60 mm and 61 mm. All intensities are normalized to one to their respective maximum.

#### 4. Results and discussion

Fig. 7 shows the resulting ablation rate against an increasing feed rate with and without the shifted beam-shaping element. As fixed parameters a pulse repetition rate of 100 kHz, a pulse length of 250 fs and a wavelength of 1030 nm were chosen. The rotation speed of the work piece was set to 500 rpm. A total of four different laser power levels at 10, 20, 30 and 40 W are investigated.

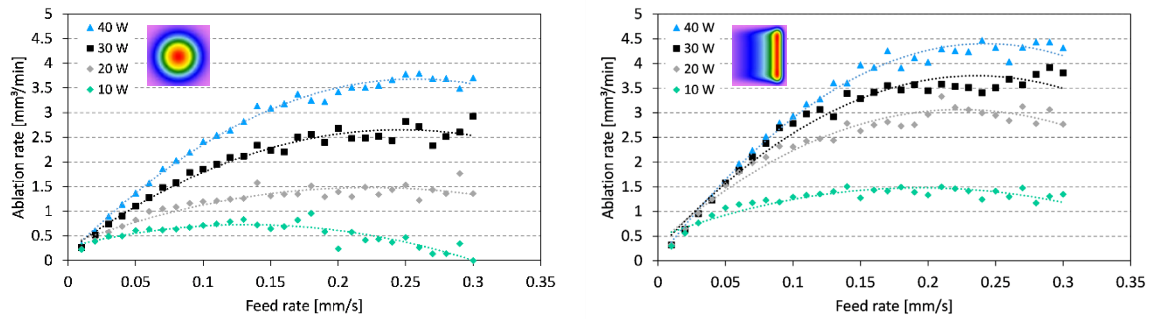


Fig. 7. Attained ablation rates for different laser powers over an increasing feed rate. Left: Gaussian beam shape (reference). Right: shifted GTH beam shaping element.

The results show that by applying the shifted beam shaping element, an increase of the ablation rate can be observed as compared to applying a Gaussian beam profile. In particular, for a laser power of 10 W the highest ablation rate achieved is  $0.96 \text{ mm}^3/\text{min}$  when using a Gaussian beam profile, whereas the highest value using the shifted GTH beam profile lies at  $1.51 \text{ mm}^3/\text{min}$ , i.e. an increase of 57.3%. For a laser power of 40 W, an increase of 17.7% in ablation rate at the respective peak values is determined. These results are underlined by the calculated process efficiencies shown in Fig. 8.

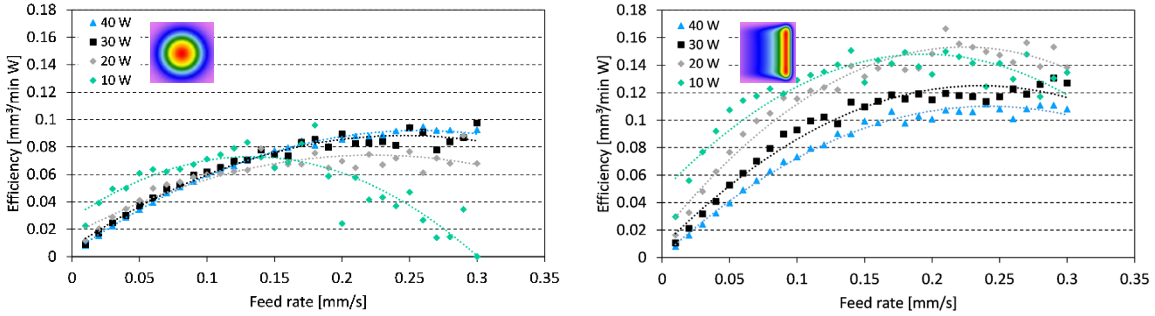


Fig. 8. Process efficiencies over increasing feed rate for different power regimes. Left: Gaussian beam shape (reference). Right: shifted GTH beam shaping element.

A significant increase in process efficiency can be observed when applying the GTH beam shape element, especially for a low average laser power. We assume that this increase in efficiency is caused by the low intensity laser irradiation of the material directly before the actual ablation process in accordance to the intensity distribution. The already excited material has a lower ablation threshold and therefore shows a better ablation behavior throughout the feeding process. In addition, due to the elongated focal spot, the material is far more often exposed to the laser throughout the feeding process, resulting, even at lower intensities, in enhanced ablation conditions. This poses a significant advantage in contrast to the Gaussian beam profile and can therefore be considered as beneficial for the overall process efficiency.

## 5. Conclusion

In this study, a beam shaping element GTH (Gaussian to Top Hat) was used to create an elongated focal spot with a one sided slowly decreasing intensity profile by a lateral shift within the beam path. Simulations and calculations of the resulting beam propagation and its intensity distribution around the focal area are presented. The beam shaping technique was applied in the laser turning process and compared to conventional Gaussian beam shape processing. The experiments show that by a lateral shift of the Gaussian to Top Hat beam shaping element a distinct increase in ablation rate, especially in the low power regime, is achieved. In particular, with a maximum value of  $1.51 \text{ mm}^3/\text{min}$ , an increase of 57.3 % at an average power of 10 W is attained. We attribute this increase to the slowly ascending laser intensity within the focal plane due to the given intensity distribution, showing an incubation effect, as well as to the elongated shape of the focal spot, which results in more frequent exposure of the material to the laser.

## Funding

German Federal Ministry of Education and Research (BMBF, FKZ 01QE1852B, Eurostars E!12423 OpEn Laserlathe)

## References

- Basler, C., Brandenburg, A., Michalik, K., Mory, D., 2019., in: "Comparison of Laser Pulse Duration for the Spatially Resolved Measurement of Coating Thickness with Laser-Induced Breakdown Spectroscopy", Sensors 19, p. 4133.
- Bischoff, C., Völklein, F., Schmitt, J., Rädel, U., Umhofer, U., Jäger, E., Lasagni, A. F., 2019., in: "Design and Manufacturing Method of Fundamental Beam Mode Shaper for Adapted Laser Beam Profile in Laser Material Processing", Materials 12, p. 2254.
- Canfield, B. K., Costa, L., Rajput, D., Terekhov, A., Lansford, K., Hofmeister, W. H., Davis, L. M., 2020., in: "Machining of micrometer-scale high aspect ratio features with single femtosecond laser pulses", Journal of Laser Applications 32, p. 32021.
- Chen, Y., Cao, Y., Wang, Y., Zhang, L., Shao, G., Zi, J., 2020., in: "Fabrication of grooves on polymer-derived SiAlCN ceramics using femtosecond laser pulses", Ceramics International 46, p. 11747.
- Dickey, F. M., Holswade, S. C., 1996., in: "Gaussian laser beam profile shaping", Optical Engineering 35, p. 3285.
- El-Khoury, M., Voisiat, B., Kunze, T., Lasagni, A. F., 2018., in: "Utilizing Fundamental Beam-Mode Shaping Technique for Top-Hat Laser Intensities in Direct Laser Interference Patterning", Journal of Laser Micro/Nanoengineering 13, p. 268.
- Goodman, J. W., in: "Introduction to Fourier optics" S. Director, Editor. McGraw-Hill, New York, p. 97.
- Hossfeld, J., Jaeger, E., Tschudi, T. T., Churin, E. G., Koronkevich, V. P.: Intl Colloquium on Diffractive Optical Elements, 1991, p. 159.
- Lickschat, P., Metzner, D., Weißmantel, S., 2020., in: "Fundamental investigations of ultrashort pulsed laser ablation on stainless steel and cemented tungsten carbide", The International Journal of Advanced Manufacturing Technology 3-4, p. 1167.
- Lutz, C., Roth, G.-L., Rung, S., Esen, C., Hellmann, R., 2021., in: "Efficient Ultrashort Pulsed Laser Processing by Dynamic Spatial Light Modulator Beam Shaping for Industrial Use", Journal of Laser Micro/Nanoengineering 16, p. 62.
- Račiukatis, G., Stankevičius, E., Gečys, P., Gedvilas, M., Bischoff, C., Jäger, E., Umhofer, U., Völklein, F., 2011., in: "Laser Processing by Using Diffractive Optical Laser Beam Shaping Technique", Journal of Laser Micro/Nanoengineering 6, p. 37.
- Ravi-Kumar, S., Lies, B., Zhang, X., Lyu, H., Qin, H., 2019., in: "Laser ablation of polymers: a review", Polymer International 68, p. 1391.
- Romero, L. A., Dickey, F. M., 1996., in: "Lossless laser beam shaping", Journal of the Optical Society of America A 13, p. 751.
- Rung, S., 2013., in: "Laserscribing of Thin Films Using Top-Hat Laser Beam Profiles", Journal of Laser Micro/Nanoengineering 8, p. 309.
- Schwarz, S., Hellmann, R., 2017., in: "Fabrication of Cylindrical Lenses by Combining Ultrashort Pulsed Laser and CO<sub>2</sub> Laser", Journal of Laser Micro/Nanoengineering 12, p. 76.
- Veldkamp, W. B., Kastner, C. J., 1982., in: "Beam profile shaping for laser radars that use detector arrays", Applied optics 21, p. 345.
- Wiegelmann, M., Dreisewerd, K., Soltwisch, J., 2016., in: "Influence of the Laser Spot Size, Focal Beam Profile, and Tissue Type on the Lipid Signals Obtained by MALDI-MS Imaging in Oversampling Mode", Journal of American Society for Mass Spectrometry 27, p. 1952.
- Xie, Q., Li, X., Jiang, L., Xia, B., Yan, X., Zhao, W., Lu, Y., 2016., in: "High-aspect-ratio, high-quality microdrilling by electron density control using a femtosecond laser Bessel beam", Applied Physics A 122, p. 136.
- Yang, J. J., Wang, M. R., 2003., in: "Analysis and optimization on single-zone binary flat-top beam shaper", Optical Engineering 42, p. 3106.
- Yang, L., Wei, J., Ma, Z., Song, P., Ma, J., Zhao, Y., Huang, Z., Zhang, M., Yang, F., Wang, X., 2019., in: "The Fabrication of Micro/Nano Structures by Laser Machining", Nanomaterials 9, p. 1789.
- Žemaitis, A., Gaidys, M., Gečys, P., Račiukaitis, G., Gedvilas, M., 2019., in: "Rapid high-quality 3D micro-machining by optimised efficient ultrashort laser ablation", Optics and Lasers in Engineering 114, p. 83.
- Zettl, J., Klar, M., Esen, C., Hellmann, R., 2020., in: "Generation of Rotationally Symmetric Micro Tools using Ultrashort Laser Pulses", Journal of Laser Micro/Nanoengineering 15, p. 118.